Effect of Filler Dimensionality on the Order−Disorder Transition of a Model Block Copolymer Nanocomposite

**Anurag Jain,[†] Jochen S. Gutmann,[†]
Carlos B. W. Garcia,[†] Yuanming Zhang,[†]
Mark W. Tate,[‡] Sol M. Gruner,[‡] and
Ulrich Wiesner*,[†]**

*Department of Materials Science and Engineering,
Cornell University, Bard Hall, Ithaca, New York 14853;
Department of Physics, Cornell University, Clark Hall,
Ithaca, New York 14853*

Introduction. The majority of commercially available polymeric materials consist of a polymer matrix whose properties are augmented by the addition of filler materials. Representative filler materials consist of carbon black or silicates.[1,2] They can have spherical, rodlike, or platelike geometry, the latter derived, for example, from clay nanoparticles.[2] Typically the fillers are used to enhance the properties of the polymer matrix, such as tensile strength, modulus, or heat distortion temperature. While in the past large fillers have often been used, industrial as well as academic research is currently focusing on nanocomposites.[3] As a result of the large surface area of nanoscopic fillers, very small amounts can induce significant changes in polymer properties. As an example, in ref 4, it has been shown that for a styrene methylvinyloxazoline copolymer matrix, the addition of as little as 5 wt % modified montmorillonite clay nanoparticles increases the tensile modulus 1.4 times.

Systematic theoretical studies of thermodynamic and dynamic properties of block-copolymer-based nanocomposites have only been conducted recently owing to their complexity.[5−11] In these simulations, the filler particles are of an ideal nature; i.e., they are completely dispersed, their geometry is very well-defined, and their surface is often taken to be either completely wettable or nonwettable by the polymer matrix. These assumptions are very difficult to realize experimentally, as it is, for example, very challenging to exfoliate the lamellae of clay type fillers completely. Thus, there is clearly a need for a model system that allows the creation of nanoscale filler materials with well-defined geometries and surface potentials.

We have recently shown that the block copolymer assisted sol−gel synthesis of silica type materials allows an unprecedented control over the shape and size of the resulting nanoparticles.[12−14] Furthermore, the surface of the silica particles is decorated with polymer chains as a consequence of their synthesis,[13] resulting in a controlled surface potential.

In the present study we use the aforementioned approach to synthesize nanoobjects with spherical, rodlike, and platelike geometry and a layer of polyisoprene hairs on their surface. These nano-objects are used as fillers in a poly(styrene-*b*-isoprene) block copolymer (PS-*b*-PI) matrix to generate model nanocomposites. In this model system, the filler particles have a well-controlled dimensionality and are preferentially wetted by the polyisoprene block of the matrix copolymer. In this first report the influence of filler dimensionality on the order−disorder phase transition of the matrix block copolymer is investigated.

Experimental Section. (a) Matrix and Filler Synthesis. Both the matrix PS-*b*-PI diblock copolymer (PS-*b*-PI), as well as the poly(isoprene-*b*-ethylene oxide) diblock copolymer (PI-*b*-PEO) used for the block-copolymer-directed filler synthesis were synthesized using anionic polymerization techniques.[15,16] Gel permeation chromatography (GPC) was used to determine the precursor molecular weight (polystyrene in the case of PS-*b*-PI and polyisoprene in the case of PI-*b*-PEO) and the dispersity of the block copolymers. ^{1}H NMR was used to determine the chemical composition of the block copolymers and the microstructure of the PI blocks. The results were used to determine the overall molecular weight of the block copolymers. The molecular parameters were determined to be M_n = 20 800 g/mol, PDI = 1.06, and f_{PS} = 0.55 for the PS-*b*-PI copolymer and M_n = 13 700 g/mol, PDI = 1.04, and f_{PEO} = 0.15 in the case of the PI-*b*-PEO copolymer. The synthesis of "hairy" silica-like fillers with spherical, rodlike, and platelike geometries was performed by a PI-*b*-PEO directed sol−gel synthesis.[13] In this process, the PEO block is swollen by ceramic precursors and acts like nanoreactors for their sol−gel synthesis. The resulting nanostructured hybrids with PI as the majority phase can be dispersed in an organic solvent to generate objects of spherical, rodlike, and platelike geometry. Since PEO acts as an anchor block inside the ceramic phase, a thin layer of PI "hairs" covers the resulting nano-objects. These hairy nano-objects were then dispersed in toluene to make a 0.1 wt % solution. A Branson 250 sonifier (tip diameter $^{7}/_{8}$ in., 60% maximum output, 50% duty cycle) was used to achieve complete separation of aggregated nano-objects.

(b) Sample Preparation. Sample specimen were obtained by solvent casting from a common toluene solution. To facilitate complete mixing, a 0.1 wt % sonicated toluene solution of the nanoscopic fillers was mixed to a PS-*b*-PI stock solution to generate nanocomposites with 0.5 wt % filler loadings. The stock solution consisted of 5 wt % PS-*b*-PI diblock copolymer and 0.0025 wt % 2,6-di-*tert*-butyl-4-methyl phenol as an anti oxidant in toluene. During casting the solvent was allowed to evaporate over a period of 2−3 days. This was followed by drying in a vacuum oven at 50 °C for 24 h and annealing at 100 °C for 24 h.

(c) SFM Imaging of Fillers. For real space imaging of the nanoscopic silica-like fillers a DI Multimode SFM was utilized. The SFM was operated in tapping mode and equipped with "Ultrasharp" NSC15/50 tips (Silicon-MDT Ltd.). The SFM samples were prepared by dip-coating a freshly cleaved mica layer in the filler solution. For ease of characterization, the polyisoprene hairs associated with the nano-objects on the SFM samples were etched away using UV−ozone treatment. The individual SFM images were corrected for nonlinearities in the scanner movement. A deconvolution of the tip shape from the images was not performed.

[†] Department of Materials Science and Engineering, Cornell University.
[‡] Department of Physics, Cornell University.

(d) Scattering Experiments. SAXS experiments were performed for macroscopic characterization of matrix, fillers and the nanocomposites derived from them. The laboratory setup consisted of a Rigaku rotating anode X-ray source (Cu Kα, 1.54 Å) operated at 46 kV, 60 mA. The X-rays were monochromated using a nickel filter and focused onto the detector using a set of Franks mirrors. A 2-D CCD detector (512 × 512 pixels)[17] at a sample to detector distance of 92.05 cm was used to record the scattering images. Images obtained from the block copolymer silicate nanocomposites consisted of isotropic rings and were integrated azimuthally for further analysis. To study the temperature dependence of the order−disorder transition of the matrix PS-*b*-PI copolymer, the samples were mounted on a heating stage with an accuracy of 0.1 °C over the investigated temperature range of 100−190 °C. Measurements were performed on heating in increments of 1−2 °C, with a typical equilibration time of 2 min.

Results and Discussion. (a) Characterization of Fillers and Matrix. Characterization of filler materials starts through the analysis of the SAXS patterns of the nanostrctured bulk hybrid materials prior to dissolution. On the basis of these experiments (data not shown), the thickness of the plates and the core diameter of rods and spheres were estimated to be 12, 14, and 18 nm, respectively. As will be shown below these values are very close to the *d* spacing of the matrix lamellar PS-*b*-PI diblock copolymer. Figure 1 shows representative SFM images of the fillers on a mica surface. These images demonstrate that the shape of the fillers is very well controlled and serve as a control of filler solutions before mixing. Typical filler dimensions (cylinders and plates) extend over several micrometers as expected from the grain structure of block copolymers used for their synthesis.[18]

The PS-*b*-PI diblock copolymer, used as the matrix for the model nanocomposite systems, was characterized by variable temperature SAXS measurements in order to determine its morphology and order−disorder phase transition temperature prior to filler incorporation. The presence of equally spaced higher order Bragg peaks in the SAXS diffractogram in Figure 2 confirms a lamellar morphology with a *d* spacing of 18.7 nm. The slightly asymmetric composition (f_{PS} = 0.55) accounts for the presence of the second order Bragg peak at $2q^*$, which would otherwise be symmetry forbidden. The inset in Figure 2 depicts the temperature dependence of the first order Bragg peak between 120 and 190 °C. A discontinuity is easily observed indicating the order−disorder transition and the transition temperature (T_{ODT}) of the matrix block copolymer. To further characterize the phase transition, the peak shape was analyzed in terms of its maximum intensity ($I(q^*)$), peak position (q^*), and full width at half-maximum (fwhm). Below the phase transition temperature a Gaussian line shape on a polynomial background was used for line shape analysis. Above the phase transition a line shape based on the structure factor of the disordered phase as derived by Leibler[19] was used. As customary in the study of the order−disorder transition phenomena of block copolymers, T_{ODT} can be obtained from the discontinuity in plots of either $1/I(q^*)$, $1/q^*$, or fwhm as a function of $1/T$.[20−22] Since all plots showed similar behavior, we will restrict our discussion to $1/I(q^*)$ vs $1/T$ curves in the following (Figure 3). For the pure PS-*b*-PI block copoly-
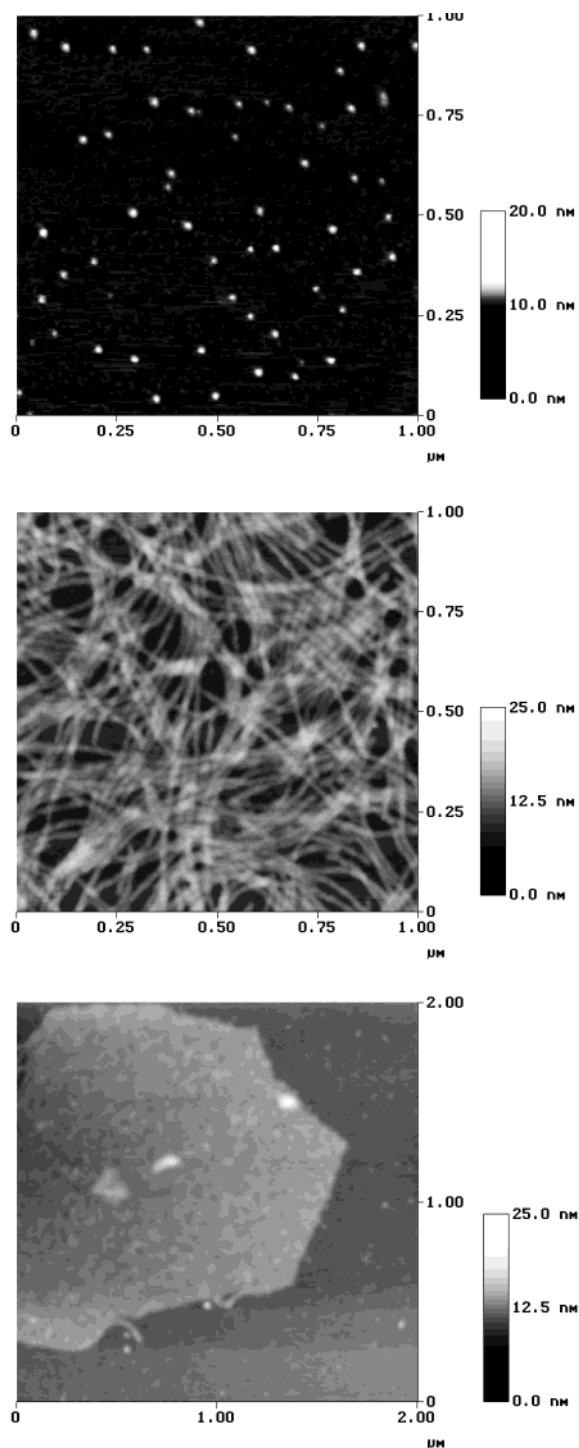

Figure 1. SFM images of the silica-type filler materials. The filler particles were plasma treated prior to imaging to remove their organic outer layer for easier imaging. Note that images do not reflect real concentrations but were chosen to show filler shapes unambiguously.

mer a well-defined discontinuity, i.e., a phase transformation at about 178 °C is observed.

(b) Characterization of Model Nanocomposites. Room-temperature SAXS experiments (Figure 2) on model nanocomposites with 0.5 wt % loading of spherical, rodlike, or platelike fillers confirmed that the lamellar morphology of the matrix is maintained in all three systems with a slight increase in the *d* spacing for the nanocomposites compared to the pure block copolymer. Figure 3 compares the plots of $1/I(q^*)$ vs $1/T$ for the model nanocomposites with that of the pure block
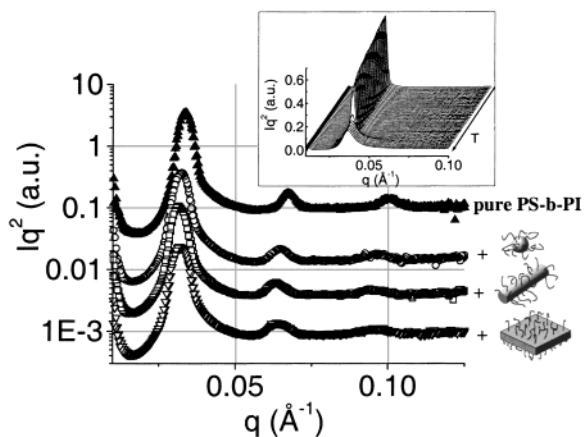
Figure 2. Small angle X-ray scattering (SAXS) diffractograms of the pure PS-*b*-PI block copolymer matrix and the three nanocomposites at room temperature. Data are shifted vertically for clarity. The integer spacing of Bragg peaks indicates lamellar morphology in all systems. Note the slightly higher values of the *d* spacing for the nanocomposites ($q^* = 0.0323$, 0.0317, and 0.0321 Å^{-1} for the nanocomposites filled with spheres, rods, and plates, respectively) compared to the pure block copolymer ($q^* = 0.0336$ Å^{-1}). The inset shows the temperature dependence of the first-order Bragg peak for the pure block copolymer over a temperature range of 120 (top) to 190 °C (bottom) in intervals of 2 °C.
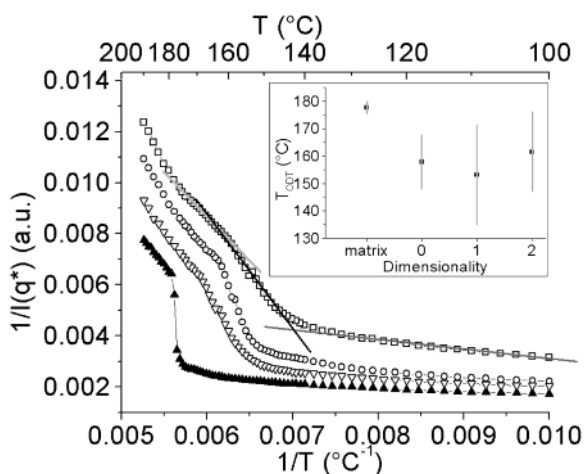

Figure 3. Comparison of the temperature-dependent intensity of the first-order Bragg peak for the bare matrix copolymer and nanocomposites containing 0.5 wt % fillers with different geometries. Data are vertically shifted for clarity. Symbols are identical to Figure 2. The procedure adopted for the determination of T_{ODT} and the phase transition temperature window is shown for the nanocomposite with rodlike fillers (see text for more information). The inset shows the dependence of the order–disorder transition temperature on the dimensionality of the fillers. The vertical bars indicate the width of the phase transition region. The pure block copolymer is denoted "matrix" and is included as a reference.

copolymer. The transitions of all three nanocomposite systems are significantly shifted toward lower temperatures. In contrast to the pure block copolymer, however, the exact location of T_{ODT} of the composites is not readily discernible from the $1/I(q^*)$ vs $1/T$ curves since the transitions are less sharp. We therefore adopted the following procedure to determine T_{ODT}. The curves were divided into three temperature regimes: significantly below, above, and close to the phase transition point. In each temperature segment, the $1/I(q^*)$ vs $1/T$ curves were approximated by a straight line (see Figure 3). The temperature range spanning the phase transition phe-

nomena was determined from the two intersections of the three lines. The actual phase transition temperature (T_{ODT}) was then taken as the midpoint of the transition temperature interval. The inset in Figure 3 summarizes the values for T_{ODT} as well as for the width of the transition obtained from this construction. It should be noted that the vertical bars in the inset are thus not representing error bars, but the actual width of transitions. To compare the influence of the filler dimensionality on T_{ODT}, the spherical, rodlike, and platelike fillers were taken to be 0-, 1-, and 2-dimensional. It is interesting to note that the depression of T_{ODT} is not a simple function of dimensionality. It shows a shallow extremum with the largest depression by about 23 °C with respect to the pure block copolymer matrix found in the nanocomposite containing rodlike fillers. The observed effects were reproduced in two separate sample sets. Subsequent heating cycles on the same sample lead to no changes in the temperature dependence of the transition. Degradation phenomena can thus be excluded. We also verified that the observed effects are not a result of free PI-*b*-PEO (leaching out of the nanoobjects) in PS-*b*-PI by preparing a PS-*b*-PI sample containing 0.5 wt % PI-*b*-PEO. No significant effect on T_{ODT} was observed in this sample, in contrast to results of a recent study of a PEO-containing triblock copolymer in PS-*b*-PI.[23]

To rationalize the results, the effect of addition of the fillers to the block copolymer matrix may be separated into two distinct contributions: energetic and geometric constraints. The energetic influence of the filler particles arises from contact interactions between the individual PS and PI blocks of the block copolymer matrix and the filler particle surface. Since the surface is covered with polyisoprene hairs, the particles are intrinsically wettable by the PI blocks of the matrix. This wettability, however, is known to impose strong geometrical constraints on the block copolymer matrix.[5] These constraints may then act as nucleation sites for the melting process, as they provide regions in which the fluctuations are much larger than usual.

For the same weight fraction, the number of filler particles increases in the following order: plates, cylinders, and spheres. Thus, on the basis of the number of structural defect sites alone, the greatest depression is expected for the spherical fillers. This is not supported by the current experimental observations. Recent computer simulations[7,9] suggest that spherical fillers can be incorporated into one block of the copolymer matrix in a fairly straightforward way. The scenario is expected to be very different for long and, in particular, flexible rods, which can induce significant structural defects. Moving from cylinders to plates, the depression in ODT decreases again because of presumably easier incorporation of these sheets in the lamellar matrix. A significant broadening of the transition temperature window suggests a scenario of inhomogeneous melting, in which the energy cost associated with the defect sites varies greatly. The rods and plates are anisotropic in nature and have a fairly broad size distribution; consequently, the defects associated with these filler particles have a broad size distribution as well. The monodisperse and isotropic nature of spherical fillers on the other hand is anticipated to induce defect sites that are all very similar, thus causing less broadening.

Conclusions. We have shown that nanoscopic silicate type fillers derived from a block copolymer assisted

synthesis constitute an interesting model system to study the properties of nanocomposites with fillers of well-defined geometry and surface properties. Using a block copolymer matrix, we have demonstrated that the addition of as little as 0.5 wt % fillers drastically alter the thermodynamic properties of the nanocomposites. The order−disorder transition temperature is lowered by 15−23 °C and is accompanied by a significant broadening of the transition temperature window. The dimensionality of the fillers plays a significant and nontrivial role in the process of the order−disorder phase transition. Rodlike fillers induce the largest depression and broadening of the phase transition. The findings are rationalized based on varying defect energy density arguments as also supported by recent computer simulations. Experimental work to further elucidate the origins of the observed behavior is now in progress in our laboratory.

References and Notes

(1) Yurekli, K.; Krishnamoorti, R.; Tse, M. F.; Mcelrath, K. O.; Tsou, A. H.; Wang, H. C. *J. Polym. Sci., Part B: Polym Phys.* **2001**, *39*, 256.
(2) Giannelis E. P. *Adv. Mater.* **1996**, *8*, 29.
(3) Giannelis E. P.; Krishnamoorti, R.; Manias, E. *Adv. Polym. Sci.* **1999**, *138*, 107.
(4) Hasegawa, N.; Okamoto, H.; Kawasumi, M.; Usuki, A. *J. Appl. Polym. Sci.* **1999**, *74*, 3359.
(5) Balazs, A. C.; Ginzburg, V. V.; Qiu, F.; Peng, G.; Jasnow, D. *J. Phys. Chem. B* **2000**, *104*, 3411.
(6) Sevink, G. J. A.; Zvelindovsky, A. V.; Vlimmeren, B. A. C.; Maurits, N. M.; Fraaije, J. G. E. M. *J. Chem. Phys.* **1999**, *110*, 2250.
(7) Thompson, R. B.; Ginzburg, V. V.; Matsen, M. W.; Balazs, A. C. *Science* **2001**, *292*, 2469.
(8) Qiu, F.; Peng, G.; Ginzburg, V. V.; Balazs, A. C.; Chen, H. Y.; Jasnow, D. *J. Chem. Phys.* **2001**, *115*, 3779.
(9) Huh, J.; Ginzburg, V. V.; Balazs, A. C. *Macromolecules* **2000**, *33*, 8085.
(10) Lee, J. Y.; Baljon, A. R. C.; Sogah, D. Y.; Loring, R. F. *J. Chem. Phys.* **1987**, *112*, 9112.
(11) Groenewold, J.; Fredrickson, G. H. *Eur. Phys. J. E: Soft Matter* **2001**, *5*, 171.
(12) Templin, M.; Franck, A.; Du Chesne, A.; Leist, H.; Zhang, Y.; Ulrich, R.; Schädler, V.; Wiesner, U. *Science* **1997**, *278*, 1795.
(13) Ulrich, R.; Du Chesne, A.; Templin, M.; Wiesner, U. *Adv. Mater.* **1999**, *11*, 141.
(14) Simon, P. F. W.; Ulrich, R.; Spiess, H. W.; Wiesner, U. *Chem. Mater.* **2001**, *13*, 3464.
(15) Hsieh, H. L.; Quirk, R. P. *Anionic Polymerization: Principles and Practical Applications*; Marcel Dekker Inc.: New York, 1996; Chapter 4.
(16) Allgaier, J.; Poppe, A.; Willner, L.; Richter, D. *Macromolecules* **1997**, *30*, 1582.
(17) Tate, M. W.; Gruner, S. M.; Eickenberry, E. F. *Rev. Sci. Instrum.* **1997**, *68*, 47.
(18) Hamley, I. W. *The Physics of Block Copolymers*; Oxford Science Pub.: Oxford, England, 1998.
(19) Leibler, L. *Macromolecules* **1980**, *13*, 1602.
(20) Fredrickson, G. H.; Helfand, E. *J. Chem. Phys.* **1987**, *87*, 697.
(21) Bodycomb, J.; Yamaguchi, D.; Hashimoto, T. *Macromolecules* **2000**, *33*, 5197.
(22) Sakamoto, N.; Hashimoto, T. *Macromolecules* **1995**, *28*, 6825.
(23) Bailey, T. S.; Pham, H. D.; Bates, F. S. *Macromolecules* **2001**, *34*, 6994.